YU ISSN 0015-3206
FZKAAA 13 (2) 109 (1981)

SURFACE AND BULK OPTICAL PHONONS AND PLASMONS IN BILAYER FILMS
II. ELECTRON REFLECTION AND ELECTRON TRANSMISSION

Z. LENAC* and R. BRAKO

»Ruđer Bošković« Institute, P. O. B. 1016,
Zagreb, Croatia, Yugoslavia

and

M. ŠUNJIĆ

Faculty of Science, P. O. B. 162 and
Institute of Physics of the University, P. O. B. 304,
Zagreb, Croatia, Yugoslavia

Received 10 November 1980

UDC 538.975

Original scientific paper

In previous article we investigated collective oscillations in bilayer films. In the present paper we apply those results to electron energy loss spectroscopy for electrons reflected from and transmitted through a bilayer system. In studying electron reflection, we emphasize surface mode excitation, especially the influence of the substrate on the electron energy loss (EEL) spectrum. In analyzing electron transmission, we pay special attention to bulk mode excitation and to the discrete nature of bulk modes in thin films. We compare the theoretical results obtained for reflection and transmission EEL spectra with some experimental data and we find that the agreement is good.

* Present address: Pedagogical Faculty, Rijeka, Yugoslavia.

1. Introduction

Electron energy loss spectroscopy (EELS) has become one of the most powerful tools for investigating both the surface and bulk properties of thin films[9,10]. When applied to multilayer systems, it also provides important information about the structure of interfaces[1-5]. General properties of long-range excitations in bilayer films were discussed in our previous article[11], here denoted by I. Now we shall be interested in EELS for electron reflection and electron transmission applied to bilayer systems.

Ritchie[1] was the first to investigate the probability of surface plasmon excitation by electrons moving through a semiinfinite metal. He described the electron as a semiclassical particle, with a well-defined momentum and position (trajectory approximation). This theory was generalized to ionic crystals[2], bilayer[3,4] and multilayer samples[5]. The reflection of low-energy electrons was also discussed in terms of collective oscillations in the system[6].

All these results[1-6] were based on the classical dielectric theory approach, which corresponds to the first term (Born approximation) in the perturbative quantum-mechanical treatment. Therefore, only single excitation probabilities were obtained. As Šunjić and Lucas pointed out[7], this approach is obviously in fault e. g. when the threshold energy of a collective excitation tends towards zero (as for surface plasmons in a thin metallic film). Starting with the Hamiltonian which was diagonalized in terms of long-range collective oscillations in a thin film and keeping the trajectory approximation, they were able to obtain an EEL spectrum which contained all multiexcitation processes. Evans and Mills[8] have shown how the full quantum-mechanical approach reproduces the results of Šunjić and Lucas in the case of high electron energy. Following I, in the present paper we generalize this theory[7] to include multilayer systems. We also point out some interesting new features related to a single thin film.

In Sect. 2 we derive an appropriate description of the EEL spectrum. We analyze the criteria for the trajectory approximation and the validity of the Poisson distribution[7] for EELS. We show that multiexcitation processes are very important whenever high energy electrons interact strongly with collective oscillations. In Sect. 3 we discuss the energy loss of electrons reflected on the surface of a bilayer system. We point out the influence of interface modes (I) on the reflected beam. Section 4 contains an analysis of the EELS of electrons transmitted through a bilayer system. We obtain a detailed summation over bulk modes and criteria for using the closure relation[7]. We investigate some important consequences arising from the finite cutoff wave vector and from the discrete nature of a z (normal-to--the-surface) component of the bulk wave vector.

In Sects. 3 and 4 we compare our theoretical results with some well-known experimental data. The agreement is good. In Sect. 5 we draw conclusions.

2. The energy loss spectrum

In order to discuss and compare our theoretical results (I) with experimental data, we calculate the EEL spectrum[9,10]. The energy loss spectrum of a moving charge can be described in a closed form when the momentum p_e and the energy

$E_e = p_e^2/2m_e$ of a charge are much higher than the momentum $\hbar k$ and the energy $\hbar\omega\,(k)$ of the excited collective mode in the system[1]:

$$E_e \ll \hbar\omega\,(k),\ p_e \ll \hbar k. \tag{1}$$

Assuming (1), we can describe the point charge (electron) by the classical trajectory $\vec{r}_e\,(t) = [\vec{\varrho}_e\,(t),\ z_e\,(t)]$. The energy loss spectrum $P\,(\omega)$ of such a particle is given by[7]

$$P\,(\omega) = \frac{1}{2\pi}\int_{-\infty}^{\infty} e^{i\omega t}\,P\,(t)\,dt. \tag{2}$$

$$P\,(t) = P_0\,\exp\left[\sum \int d\vec{k}\,\frac{1}{\hbar^2}\,|\,I_i\,(\vec{k})\,|^2\,e^{-i\omega_i(k)\,t}\right]. \tag{3}$$

$$I_i\,(\vec{k}) = \int_{-\infty}^{\infty} dt\,e^{i\,[\vec{k}\,\vec{\varrho}_e\,(t) - \omega_i\,(k)\,t]}\,\Gamma_i\,[\vec{k},\ z_e\,(t)]. \tag{4}$$

Here ω_i is the eigenfrequency of the i-th mode (collective oscillation) of the system and Γ_i is the coupling function of the i-th mode interacting with the external charge. A complete description of ω_i and Γ_i for a bilayer system is given in I. The normalization of the energy loss spectrum

$$\int_{-\infty}^{\infty} P\,(\omega)\,d\omega = 1 \tag{5}$$

gives the following expression for the no-loss line:

$$P_0 = \exp\left[-\sum_i \int d\vec{k}\,\frac{1}{\hbar^2}\,|\,I_i\,(\vec{k})\,|^2\right]. \tag{6}$$

$P\,(\omega)$ can be easily expanded in terms of $|\,I_i\,(\vec{k})\,|^2$, e. g.

$$P\,(\omega) = P_0\,\delta\,(\omega) + \sum_{l=1}^{\infty} P_l\,(\omega). \tag{7}$$

The zeroth term $P_0\,(\omega)\,\delta\,(\omega)$ gives the no-loss line, while the first term

$$P_1\,(\omega) = P_0 \sum_i \int d\vec{k}\,\frac{1}{\hbar^2}\,|\,I_i\,(\vec{k})\,|^2\,\delta\,[\omega - \omega_i\,(k)] \tag{8}$$

$$= P_0 \sum_i \sum_j \frac{2\pi\,k_i'}{|\,\partial\omega_i\,(k_i')/\partial k\,|}\,\frac{1}{\hbar^2}\,|\,I_i\,(k_i')\,|^2$$

gives the (classical) probability of one-plasmon (one-optical phonon) excitation. Here k_i' is (implicitly) defined by $\omega_i\,(k_i') = \omega$ and j is the multiplicity of the solution.

In our model, bulk excitations are dispersionless, which leads to the appearance of δ-peaks in the EEL spectrum at $\omega = \omega_{Ln}$; $n = 1, 2$ denotes the plates of the system, as described in I. For surface modes, the probability $P_1(\omega)$ is proportional to the density of states $|\partial\omega_l(k_l')/\partial k|^{-1}$ times $|I_l(k_l')|^2$. The density of states tends to infinity for $\omega_l \to \omega_l(k \to \infty)$, and we expect sharp maxima close to the asymptotic frequencies of surface modes. However, the maximum at $\omega_l(k \to \infty)$ is rather weak if $|I_l(k_l')|$ has a peak far from $\omega_l(k \to \infty)$, i. e. in the strong-dispersion region. Strong dispersion is a feature of very thin films and we expect the broadening of the maxima at $\omega_l(k \to \infty)$ and even the appearance of new peaks[18].

We have neglected the intrinsic dispersion and the finite lifetime of both the surface and bulk modes. These microscopic effects can be incorporated in our theory only *a posteriori* (I). However, in high-energy electron experiments, these effects cannot be distinguished, but only lead to the broadening of spectral lines. We can neglect them when calculating the total strength of a line, but when calculating e. g. $P_1(\omega)$ we have to replace the δ-function by the Lorentzian of finite width which is, in fact, determined mainly by the resolution of the analyzer.

The probability $P(\omega)$ of l-th order processes satisfies the recursive relation

$$P_l(\omega) = l \int \mathrm{d}\omega' \, P_{l-1}(\omega') \, P_1(\omega - \omega')/P_0, \quad l > 1 \tag{9}$$

and $P_1(\omega)/P_o$ is given by (8). The expansion (7—9) is much more appropriate for numerical calculations than the equivalent expansion in Ref. 7. Still, we wish to obtain some approximate but analytic result for $P(\omega)$.

We first notice that $P_l(\omega)$ has a maximum close to $\omega = \omega_{Ia}$. Here the index a refers to the different frequencies in the system, i. e. $a = s = 1, 2, \ldots, S$ for surface modes and $a = L_1, L_2$ for bulk modes. The index I denotes the asymptotic frequency:

$$\omega_{Ia} = \begin{cases} \omega_S(k \to \infty) = \omega_{\infty s}, \; s = 1,2,\ldots,S, & \text{surface modes} \\ \omega_{L1}, \omega_{L2} & \text{, bulk modes.} \end{cases} \tag{10}$$

In the first approximation, we can exchange ω_l by ω_{Ia} in the oscillatory term $\exp[-\omega_l(k)\,t]$ in Eq. (3). This is satisfactory for bulk modes, but for surface modes we have to introduce a wave vector $\vec{\varkappa}_s$ after which this approximation holds. Assuming $\omega_s(\varkappa > \varkappa_s) \approx \omega_{\infty s}$, we define $\varkappa_s$ by

$$|\omega_s(\varkappa_s) - \omega_{\infty s}| = 0.05\,\omega_{\infty s}. \tag{11}$$

In a thin film of thickness a, one has $\varkappa_\pm \approx 1/a$[7]. Now we define the interaction strength of a surface mode s by

$$A_S^s = \int\limits_{k > \varkappa_s} \mathrm{d}\vec{k} \, \frac{1}{\hbar^2} |I_S^s(\vec{k})|^2. \tag{12}$$

The bulk modes in the plate $n = 1$ (2) all have the same frequency ω_{Ln}, so we define the strength of bulk modes by

$$A_B^n = \int \mathrm{d}\vec{k} \frac{1}{\hbar^2} |I_B^n(\vec{k})|^2 \tag{13}$$

$$|I_B^n(\vec{k})|^2 = \sum_q |I_B^q(\vec{k})|^2$$

where $q = (\pi/z_o)\, m$, $m = 1, 2, 3...$ and $z_0 = a, b$ if $n = 1, 2$, respectively (I).

Using (12) and (13), we find[7] that

$$P(\omega) \approx \Delta(\omega) + S(\omega). \tag{14}$$

The main contribution arises from $\Delta(\omega)$, which gives the standard Poisson distribution for EELS:

$$\Delta(\omega) = \sum_{n_1} \ldots \sum_{n_M} P_{n_1 \ldots n_M}\, \delta\left[\omega - \sum_{\alpha=1}^{M} n_\alpha \omega_{I\alpha}\right]. \tag{15}$$

Here $\mathrm{M} = \mathrm{Max}(\alpha)$, i. e. $\alpha = (s = 1,...,S; L_1, L_2) \equiv (1, 2,..., M)$, and $P_{n_1 \ldots n_M}$ denotes the probability of the extitation of n_α collective modes with frequency ω_α:

$$P_{n_1 \ldots n_M} = P_0 \frac{(A_{\alpha=1})^{n_1}}{n_1!} \ldots \frac{(A_{\alpha=M})^{n_M}}{n_M!}.$$

$S(\omega)$ represents the background for the sharp peaks in $\Delta(\omega)$, which is due to the strong dispersion of surface modes ($\varkappa_s > 0$):

$$S(\omega) = \sum_{n_1} \ldots \sum_{n_M} P_{n_1 \ldots n_M}\, S'\left[\omega - \sum_{\alpha=1} n_\alpha \omega_\alpha\right] \tag{16}$$

where we define

$$S'(\Omega) = \frac{1}{2\pi} \int_{-\infty}^{\infty} \mathrm{d}t\, \mathrm{e}^{\mathrm{i}\Omega t} [\mathrm{e}^{F(t)} - 1]$$

$$F(t) = \sum_s \int_{k<\varkappa_s} \mathrm{d}\vec{k} \frac{1}{\hbar^2} |I_S^s(\vec{k})|^2\, \mathrm{e}^{-\mathrm{i}\omega_s(k)t}.$$

Although $S(\omega)$ is a very complicated function, we find

$$\int S(\omega)\, d\omega = 1 - \exp[-F(0)] \tag{17}$$

and the total contribution of the background can be easily evaluated.

To find out when $S(\omega)$ can be neglected, we define $\vec{k}_{Ia}$ as a wave vector at which $|I_a(\vec{k})|$ has a maximum. This obviously happens when the phase velocity of collective oscillations ω_a/k is (roughly) equal to the charge velocity v_e, i. e.

$$k_{Ia} \approx \omega_a(k_{Ia})/v_e \approx \omega_{Ia}/v_e. \tag{18}$$

The last relation is valid only if the dispersion $\omega_a(k)$ is not too strong. According to (12) and (17), $S(\omega)$ becomes important for $\varkappa_s > k_{Is}$. Thus, the Poisson distribution satisfactorily describes the EEL spectrum if $\varkappa_s < k_{Is}$ ($\int S(\omega)\,\mathrm{d}\omega < 0.01$), i. e. if the film is not very thin and if the charge is not very fast.

The coupling of the collective oscillation (ω_a) to the external charge can be described as weak or strong, depending on whether $A_a < 1$ or $A_a > 1$, respectively (12, 13). In weak coupling, multiexcitation processes of the ω_a mode are negligible. However, for strong coupling, the most favourable process is the n_a multiexcitation process at which $A_a^n a/n_a!$ reaches its highest value (15). In this case, the classical treatment[1-6] obviously fails.

Collective oscillations are well defined only in the long-range limit. As is described in I, if we introduce a three-dimensional wave vector of collective modes by $\vec{K} = \vec{k} + q\hat{z}$, these modes are well defined for $K < K_c$, where $\vec{K}_c(\vec{k}_c, \vec{q}_c)$ is an (averaged) three-dimensional cutoff wave vector and k_c, q_c are (averaged) surface and bulk cutoff wave vectors in the direction parallel and perpendicular to the surface, respectively. We take the simplest choice, $k_c = q_c = K_c$, i e. we assume the sphere $k^2 + q^2 = K_c^2$ to be the limit of our continuous approximation. By introducing $q_c = \pi N/z_0$, we perform the summation over $q = \pi m/z_o$ to $m \leq N = K_c z_o/\pi$. Then we integrate over $\vec{k}$ i) for surface modes ($q = 0$) up to $k \leq K_c$ and ii) for bulk modes ($q > 0$) up to

$$k \leq k_0, \text{ where } k_0^2 = K_c^2 - q^2 \geq 0.$$

The condition $N \geq m \geq 1$ implies that $z' = \pi K_c^{-1}$ is the limiting film thickness below which bulk collective oscillations cannot exist. However, $\pi K_c^{-1} \approx$ (3—5) 10^{-8} cm corresponds to the distance between atomic layers in a crystal. Therefore, by introducing q_c, even our continuous model partly takes into account the discrete structure of a thin film: If it is only a monolayer, it cannot possess bulk collective oscillations.

Let us note that the summation over bulk modes can also be performed with the help of the closure relation (I, 7). This procedure assumes an infinite summation over m, i. e. $q_c \to \infty$. Therefore, it can be correct only for $N \gg 1$, i. e. for rather thick films.

If we carefully analyze the validity of the trajectory approximation (1), we find that $k_e \approx 0.5\,[E_e(\mathrm{eV})]^{1/2} \times 10^8\ \mathrm{cm}^{-1}$, $k \leq K_c \approx 10^8\ \mathrm{cm}^{-1}$, so the requirement $k \ll k_e$ holds for $E_e \gtrsim 1$ keV. Such energies are appropriate for investigating plasmons ($\hbar\omega_P \sim 10$ eV), but are much too high for detecting phonons ($\hbar\omega_L \sim$ ~ 0.1 eV). However, according to (18), it is enough to require $k_{Ia} \ll k_e$. We find $k_e/k_{Ia} \approx 2E_e(\mathrm{eV})/\omega_{Ia}(\mathrm{eV})$, so the trajectory approximation (1) holds if only one

condition, namely $E_e \gtrsim 10\hbar\omega_{Ia}$, is satisfied. Such energies are used in many experiments when investigating plasmons and optical phonons in single or multilayer films, so our theory can be easily applied and verified.

3. *Electron reflection*

The energy loss spectrum of reflected electrons is an important tool for investigating the properties of both the reflecting surface and the interface in a bilayer system. From the dielectric theory we obtain coupled surface oscillations in multilayer films (I). Comparison between the expected results and the experimental data can provide us with the important information about the surface structure[15]. For simplicity, we shall apply the results of Sect. 2 only to an electron beam specularly reflected from plate 1 of a bilayer system. In this section we concentrate on surface excitations and neglect the penetration of electrons into the sample, which is correct for small incidence angles and relatively low electron energies. Otherwise, bulk excitations may be important, but they are usually recognized in the EEL spectrum.

The electron trajectory is given by

$$\varrho_e(t) = v_{||}\, t,\ z_e(t) = v_\perp |t| + a \tag{19}$$

where the parallel and normal components of the electron velocity $\vec{v}_e \equiv \vec{v}$ are $v_{||} = v\cos\Psi$, $v_\perp = v\sin\Psi$, and Ψ is the electron incidence angle, measured from the surface. Inserting (19) into (4), we obtain from (12)

$$A_S^s = \int_{\varkappa_s}^{k_c} \mathrm{d}k\, D_s(k)\, R_s(k) \tag{20}$$

where

$$D_s(k) = \frac{1}{(2\pi)^3}\frac{e^2}{\hbar}\, v_\perp^2\, \frac{k^2\, C_S^s(k)^2}{\omega_s(k)} \tag{21}$$

$$R_s(k) = \int_0^{2\pi} \mathrm{d}\varphi\, [k^2 v_\perp^2 + (kv_{||}\cos\varphi - \omega_s(k))^2]^{-2}. \tag{22}$$

After angular integration, we find that

$$R_s(k) = 2\pi\, \frac{|r - 1 + 4u_\perp^2\,(1+u^2)/r + u^2\cos 2\Psi|}{\omega_s^4\, u_\perp^2\, r^2\, |\, 8\,(r+1-u^2)\,|^{1/2}}$$

with

$$u_{(\perp,||)} = u_s(k)_{(\perp,||)} = kv_{(\perp,||)}/\omega_s(k)$$

$$r \equiv r_s(k) = [(u_s^2 - 1)^2 + 4u_{s\perp}^2]^{1/2}.$$

The limiting values are as follows:

i) grazing incidence ($\Psi \to 0$)

$$R_s(k) \to \begin{cases} [(kv_\perp)^3 (k^2v^2 - \omega_s^2)^{1/2}]^{-1}, & k > k_{Is} \\ 0 \quad , & k < k_{Is} \end{cases}$$

ii) normal incidence ($\Psi \to \pi/2$)

$$R_s(k) \to 2\pi [k^2v^2 + \omega_s^2]^{-2}.$$

For grazing angles of incidence, $R_s(k)$ has a sharp maximum at $k_{Is} = \omega_s(k_{Is})/v \approx \omega_{\infty s}/v$ (Fig. 1), in agreement with (18), which occurs because the electron follows a long path close to the surface and interacts strongly with surface excitations. When Ψ increases, the maximum decreases and finally at $\Psi \to \pi/2$, when the electron leaves the surface quickly, $R_s(k)\, D_s(k)$ has a very smooth maximum at k_{Is} (Fig. 1).

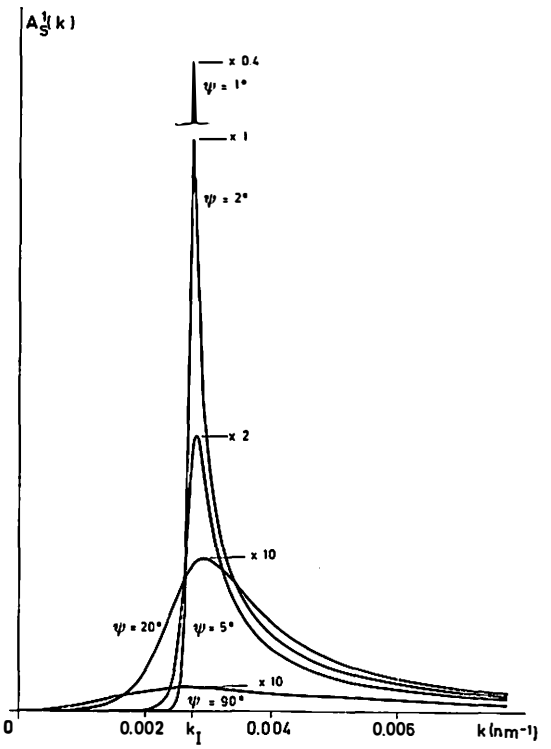

Fig. 1. The integrand $A_S^{\frac{1}{2}}(k) = D_S(k)\, R_S(k)$ for semiinfinite Al, at $E_e = 10$ keV. $A_S^{\frac{1}{2}}(k)$ reaches its maximum value at $k = k_I = \omega_\infty/v$ for all incidence angles Ψ.

Before analyzing bilayer systems in more detail, we shall briefly discuss the electron reflection on a semiinfinite plate and on a thin film. Some important features will be pointed out mainly to make more evident the comparison between the present theory and adequate experiments.

a) *Electrons reflection on a semiinfinite plate*

A semiinfinite plate has a simple solution

$$D_1(k) \equiv D_\infty = (e^2 \omega_P^2 v_\perp^2 k^2)/(2\pi \hbar \omega_\infty). \tag{23}$$

The surface mode

$$\omega_1 \equiv \omega_\infty = [(\varepsilon_\infty \omega_L^2 + \omega_T^2)/(\varepsilon_\infty + 1)]^{1/2}$$

is dispersionless ($\varkappa_\perp = 0$) and the whole spectrum is given by (15). Figure 1 shows the integrand (20) $A_S^1(k) = D_1(k) R_1(k)$ for various incidence angles. The integration over k can be performed analytically[6] to yield

$$A_S^1 = A_\infty = A_0 (\pi/2) \Upsilon(k_c)$$

where

$$A_0 = \frac{\pi}{4} \frac{e^2}{\hbar} \frac{\omega_P^2}{\omega_\infty^2} \frac{1}{v_\perp} \sim \frac{1}{\sqrt{E_e} \sin \Psi} \tag{24}$$

$$\Upsilon(k) = |\text{arc tg}\,[(r + u^2 - 1)/2]^{1/2} - (u_\perp/r)\,[(r - u^2 + 1)/2]^{1/2}|.$$

The limiting values are the following:

i) grazing incidence ($\Psi \to 0$)

$A_\infty \approx (2A_0/\pi)$ arc cos (k_1/k_c)

ii) normal incidence ($\Psi \to \pi/2$)

$$A_\infty \approx (2A_0/\pi)\,|\,\text{arc tg}\,(k_c/k_1) - (k_c k_1)/(k_c^2 + k_1^2)\,|.$$

Here we put $k_{11} \equiv k_1 = \omega_\infty/v$ and assume $k_c > k_1$. For $k_c < k_1$, the limiting values (i) and (ii) are not correct. However, then we find $E_e \lesssim [\omega_\infty\,(\text{eV})/4]^2$, and the trajectory approximation (1) is no longer valid. In the limit $k_c \gg k_1$, we find $A_\infty \approx A_0$ for all Ψ. According to (24), small values of $v_\perp \sim E^{1/2} \sin \Psi$ favour higher-order excitation processes, while large values of $v_\perp$ lead to $P_0 \approx 1$.

Figure 2 shows the probability of multiplasmon losses as a function of electron energy and incidence angle for a semiinfinite Al plate ($\omega_P \approx 15.0$ eV, $k_c \approx 1.3 \times \times 10^8$ cm^{-1}). As shown in the figure, the meaning of the probabilities $P_n/P_0 = (A_S)^n/n!$ (15) is that they simply measure the intensities of spectral lines relative to the no-loss line. Our approach would be quite correct if P_0 were replaced by the real reflectivity for elastic electron scattering[8]. However, the relative compari-

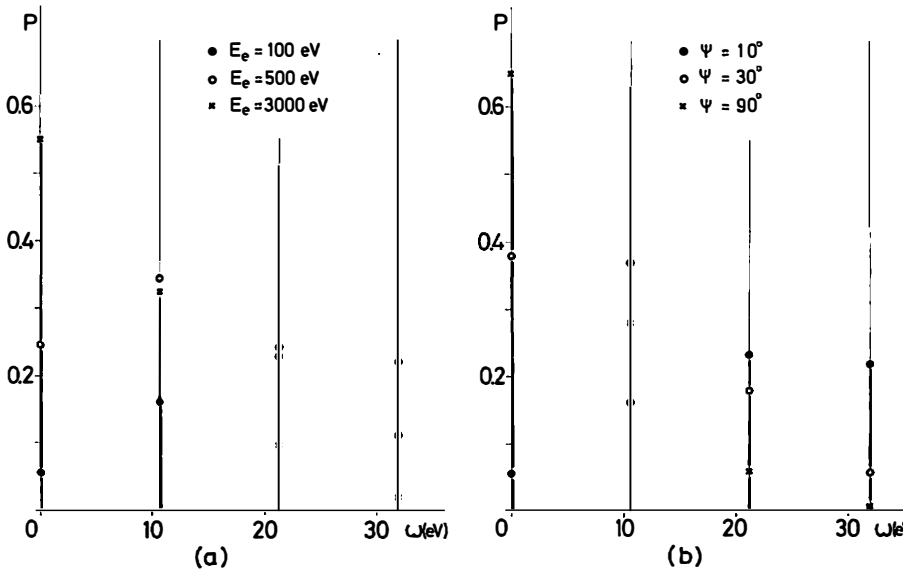

Fig. 2. Excitation probability for semiinfinite Al, as a function of a) electron energy E_e ($\Psi = 10°$), b) incidence angle Ψ ($E_e = 100$ eV).

son between the different spectral lines is independent of P_0, and thus the whole spectrum retains the same shape. With this restriction, the theoretical results for the Al plate are in good agreement with experiment[12].

b) *Electron reflection on a thin film*

There are two surface modes $\omega_s = \omega_\perp$ in a thin film with the same asymptotic frequency ω_∞. From (21) we find

$$D_{\pm}(k) = (e^2 \omega_P^2 v_\perp^2 k^2)\, e^{-ka}\, \mathrm{sh}\,(ka)/[2\pi\hbar\, \omega_\perp(k)].$$

If the dispersion is not very strong ($\varkappa < \varkappa_{IS}$), we roughly estimate from (20) that

$$A_S = A_S^+ + A_S^- \approx A_\infty |1 - (2\varkappa_S/\pi k_I)|$$

where $\varkappa_S = (\varkappa_+ + \varkappa_-)/2 \approx 1/a$, and A_∞ is given by (23). The influence of the dispersion ($\varkappa_S > 0$) leads to $A_S < A_\infty$.

Figure 3 shows the spectrum $P_1(\omega)$ of the surface plasmon excitation for a thin Al film. The Lorentzian halfwidth is taken to be $\approx 5\%\ \omega_\infty \approx 0.5$ eV. Although we find that $A_S \ll A_\infty$ for a very thin film ($a = 5 \times 10^{-8}$), the no-loss line P_0 for such a film is also much weaker than in a semi-infinite plate. The reason for that is a strong electron coupling to both surface modes of a thin film, particularly to ω_-. This coupling reaches its maximum in the strong-dispersion region ($k_I < \varkappa_S$), which implies a considerable growth of the background (16) ($\int S(\omega)\, d\omega \approx$

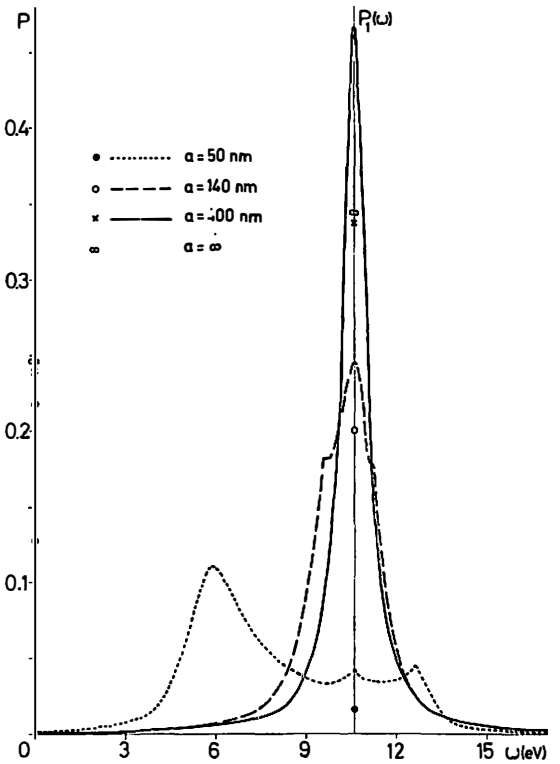

Fig. 3. The spectrum $P_1(\omega)$ (in arbitrary units) of surface plasmon excitation in a thin Al film. The corresponding excitation probabilities P_0 and P_1 are also shown. We have chosen $E_e = 500$ eV, $\Psi = 10°$.

≈ 0.8). The Poisson distribution becomes meaningless: There are two peaks instead of one, both have been detected experimentally[18].

For thicker films ($a = 14 \times 10^{-6}$ cm), both maxima are of the same intensity and ($a = 50 \times 10^{-6}$ cm) approach the same asymptotic frequency ω_∞. The background becomes negligible for $a \gtrsim 50 \times 10^{-8}$ cm ($\int S(\omega)\, d\omega \approx 0.01$), and the EEL spectrum is well described by the Poisson distribution (15).

The sharpness of the peak at ω_∞ depends, besides on the film thickness, also upon the electron energy E_e and the angle of incidence Ψ. At large E_e and Ψ, the wave vectors in the strong-dispersion region are strongly excited, which obviously broadens the peak at ω_∞. To conclude, the necessary conditions for the Poisson distribution are $k_1 > \varkappa_S$, i. e. $a > v/\omega_\infty$[7], and rather small Ψ (the allowed values dependend upon the previous condition, i. e. at $a \gg v/\omega_\infty$, the Poisson distribution holds for all Ψ). This means that the Poisson distribution holds for a sharp peak at ω_∞, when the difference between the electron reflection on the thin film and on the semiinfinite substrate becomes negligible.

c) *Electron reflection on a thin film with a semiinfinite substrate*

When one applies EELS to a sample containing two different media, the situation becomes much more complicated. Interface modes are of particular interest, because they reflect the properties of both media, and we shall carefully analyze their influence on the EEL spectrum. There are two interface modes (one, when two metals are considered) connected with the $z = 0$ surface and one mode connected with the reflecting surface $z = a$ (I). The latter mode obviously exhibits the strongest interaction with the scattered electron and we call it the dominant mode. Also, the longitudinal interface mode is usually more strongly coupled to the electron than the transverse interface mode (I). Here we give some rough but illustrative calculations.

A) *The dominant mode*: $\omega_1 (ka \gg 1) \to \omega_{\infty 1}$

In the first approximation,

$$D_1 (k) \approx D_{\infty 1} \text{ for } ka \gg 1.$$

Then for small Ψ (such that $D_1 (k) R_1 (k)$ has a sharp maximum at k_{f1}), we find

$$A_1 \approx A_{\infty 1}. \tag{25}$$

Obviously, the electron interaction with the dominant mode is approximately the same as its interaction with the surface mode ($\omega_{\infty 1}$) of the semiinfinite plate 1.

B) *Interface modes*: $\omega_{2,3} (ka \gg 1) \to \omega_{\infty 2,3}$

For interface modes, we obtain

$$D_{2,3} (k) \sim D_{\infty 2,3} \exp (-2ka) \text{ for } ka \gg 1$$

where $D_{\infty l}$ is given by (23) with $\omega_\infty \to \omega_{\infty l}$. Then, for small Ψ, we have

$$A_{2,3} \sim A_{\infty 2,3} \exp (-2\omega_{\infty 2,3}\, a/v). \tag{26}$$

By comparing (25) and (26), we find

$$A_{2,3}/A_1 \sim \exp (-2\omega_{\infty 2,3}\, a/v)$$

which means that we can detect the electron-interface mode interaction only if $\omega_{\infty 2,3}\, a/v \lesssim 1$. Obviously, the influence of the substrate is important when one deals with thin films and high electron energies. It usually corresponds to the high-dispersion region ($k_{f2,3} \lesssim \varkappa_{2,3}$). However, in some cases the Poisson distribution still holds, because the semiinfinite plate can markedly reduce the dispersion of surface in a thin film.

Figure 4 shows the spectrum $P_1(\omega)$ for the surface plasmon excitation of a thin Al_2O_3 film on an Al substrate. In the plasmon energy range, Al_2O_3 is described as an inert dielectric with $\varepsilon \approx 4$[13,19]. The increase of Al_2O_3 thickness broadens and gradually shifts the sharp maximum at $\omega_1 = \omega_P/\sqrt{2}$ ($a = 0$) towards $\omega_2 = \omega_P/\sqrt{1+\varepsilon}$ ($a > v/\omega_P \approx 7 \times 10^{-8}$ cm). At the same time, the peak becomes weaker since the surface plasmon is connected to the Al and not to the (Al + Al_2O_3) reflecting surface. The same behaviour has been observed in experiment[13]. The bulk plasmon has also been detected experimentally[12,13], because at large incidence angles the electron penetrates through the Al_2O_3 film and reaches the Al substrate.

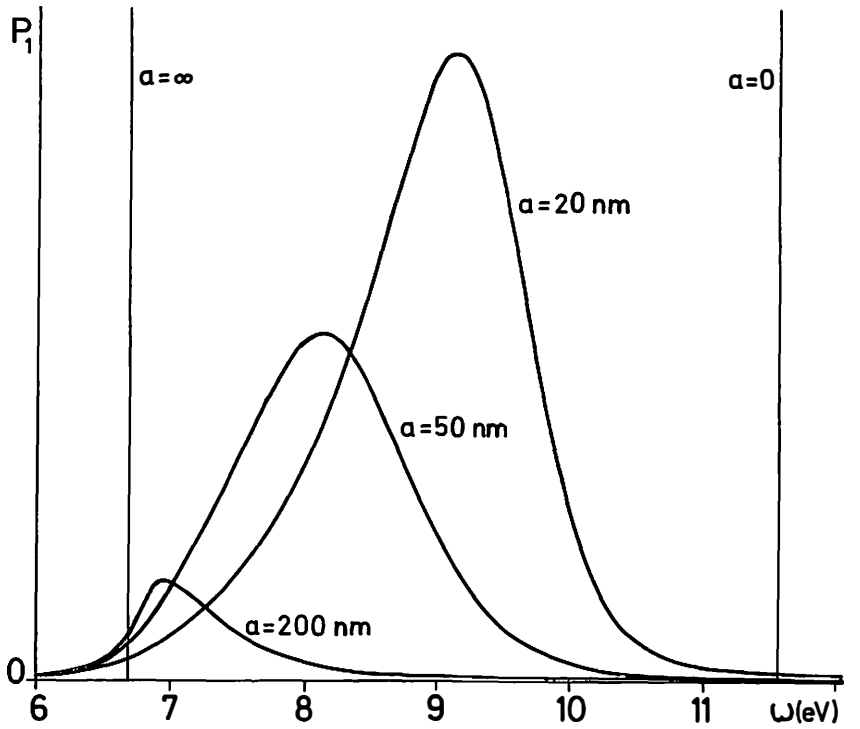

Fig. 4. The spectrum $P_1(\omega)$ of surface plasmon excitation in a thin Al_2O_3 film on semiinfinite Al. Experimental data are $E_e = 750$ eV, $\Psi = 45°$[13].

As another example we analyze a thin Al film on a CdSe substrate. Brillson[15] has shown that the position of the experimental peak and the prediction of the dielectric theory are in good agreement. We were also able to analyze the peak intensities and our results are in good qualitative agreement with experiment (Fig. 5a). A direct comparison is not possible because the experimental data[15] represent the second-derivative spectra of backscattered electrons.

The dielectric function of CdSe is given by[14,15] $\varepsilon = (\omega_L^2 - \omega^2)/(\omega_T^2 - \omega^2)$, with $\omega_L \approx 17.2$ eV, $\omega_T \approx 7.2$ eV. Two surface modes with the asymptotic frequencies $\omega_{a3} \approx 4.7$ eV, $\omega_{a2} \approx 16.3$ eV are connected with the interface, and one surface mode is related to the free surface ($\omega_{a1} \approx 10.6$ eV) (15, I).

We analyze the excitation probability of one surface mode P_1 as a function of Al film thickness (Fig. 5a), electron energy (Fig. 5b) and angle of incidence (Fig. 5c). In agreement with experiment (Fig. 5a), the excitation probability of an interface mode is significant only for very thin Al films ($a \lesssim \omega_P \approx 3 \times 10^{-8}$ cm) and decreases rapidly for thicker Al films (25, 26), ii) the excitation probability of the ω_3 mode is much greater than of the ω_2 mode and iii) the dominant mode (ω_1) almost completely screens the interface modes at $a \lesssim 20 \times 10^{-8}$ cm. Note that the electron penetration into the system leads to the bulk Al plasmon excitation.

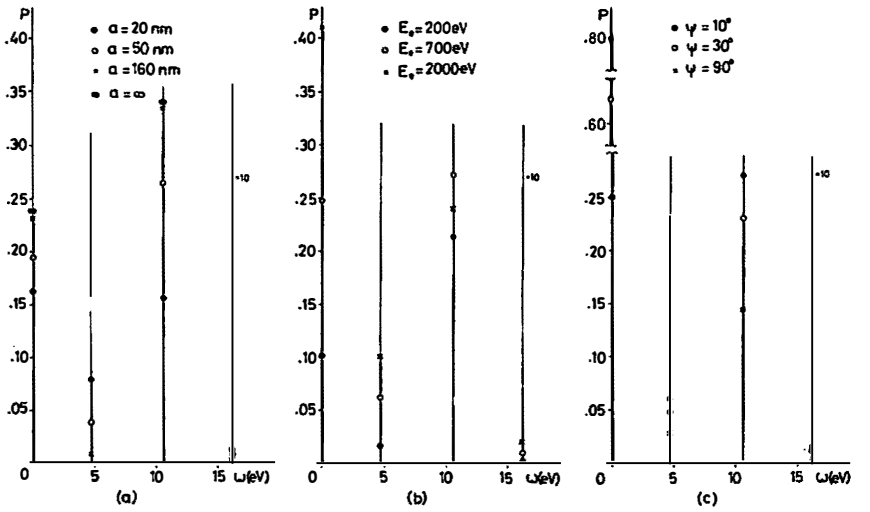

Fig. 5. Excitation probability for a thin Al film on a CdSe substrate, as a function of a) Al film thickness a ($E_e = 100$ eV, $\Psi = 20°$), b) electron energy E_e ($a = 10^{-7}$ cm, $\Psi = 10°$), c) incidence angle Ψ ($a = 10^{-7}$ cm, $E_e = 700$ eV).

The increase of electron energy (Fig. 5b) also leads to the (relative) increase of interface mode excitation probability, while for the dominant mode, P_1 first increases and then ($v_\perp \gtrsim e^2/\hbar$) decreases. Therefore, high electron energies are convenient for the investigation of interface modes.

The excitation probability of the dominant mode (ω_1) and of the interface mode (ω_2) decreases with increasing incidence angle Ψ (Fig. 5c). However, the ratio of these two lines remains roughly constant at all incidence angles.

d) *Electron reflection on two thin films*

In two thin films (I), the dominant mode and the interface modes follow the same approximate relations as in c).

C) *The weak mode*: $\omega_4 (kb \gg 1) \to \omega_{\infty 4}$

The new surface mode $\omega_4 (k)$ is connected to the new surface $z = -b$. Therefore, it interacts weakly with the electron reflected on the surface $z = a$; this interaction obviously vanishes at $b \to \infty$. In the limit $kb \gg 1$, we find

$$D_4 (k) \sim D_{\infty 4} \exp [-2k (a + b)].$$

Then (for small Ψ) we roughly estimate

$$A_4 \sim A_{\infty 4} \exp\left[-2\omega_{\infty 4}(a+b)/v\right] \tag{27}$$

so the weak mode can be detected only for $\omega_{\infty 4}(a+b)\, v \lesssim 1$, i. e. both films should be very thin. Even in this case, the electron interaction with the interface and especially with the dominant mode mostly screens the interaction with the weak mode. In a good approximation, one can treat the electron reflection on two thin films as the electron reflection on film 1 placed on a semiinfinite substrate 2.

Let us note that Brillson observed one additional surface mode in the Al-CdSe system[15]. He connected this mode to a very thin ($\approx 4 \times 10^{-8}$ cm) film which appeared at the Al-CdSe interface. Although an optically active film introduces two new modes, the electron interacts again strongly only with one of them. In agreement with (27), the excitation probability of the new mode decreases rapidly with increasing Al thickness.

4. *Electron transmission*

When an electron is transmitted through a bilayer film, it excites both surface and bulk collective oscillations. The EEL spectrum of bulk excitations in a thin film can give us, e. g. a direct insight into the discrete nature of bulk collective modes. For simplicity, we analyze the normal incidence only, so the electron trajectory is given by

$$\vec{\varrho}_e(t) = 0, \quad z_e(t) = -vt. \tag{28}$$

The interaction strength of surface and bulk modes follows from (12) and (13):

i) *Surface modes*

$$A_s^s = \int_{\varkappa_s}^{k_c} \mathrm{d}k\; T_s(k)\, |\mathcal{J}_s(k)|^2 \tag{29}$$

where we have used the notation

$$T_s(k) = \frac{e^2}{\hbar}\frac{1}{v^2}\frac{1}{\omega_s(k)}\frac{k^2}{(k^2+\alpha_S^{s2})^2} \tag{30}$$

$$\mathcal{J}_s(k) = \frac{C_S^s}{2\pi\sqrt{k}}\frac{(k^2+\alpha_S^{s2})}{2k}\int_{-\infty}^{\infty}\mathrm{d}z\; \mathrm{e}^{\mathrm{i}\alpha_S^s z}\,\gamma_S^s(k,z) \tag{31}$$

$$= \frac{C_S^s}{2\pi\sqrt{k}}\left[-C_4^s\,\mathrm{e}^{(k-\mathrm{i}\alpha_S^s)b} + C_1^s\,\mathrm{e}^{(k+\mathrm{i}\alpha_S^s)a} + C_4^s - C_2^s\right].$$

Here $\alpha_S^i \equiv \alpha_S^i(k) = \omega_s(k)/v$, and γ_S^i, together with the coefficients $C_i \equiv C_i(k)$, are defined in I.

ii) *Bulk modes*

$$A_B^n = \frac{e^2}{z_0} \frac{1}{\hbar \omega_{Ln}} \frac{\omega_{Pn}^2}{v^2} \sum_q f_q^{\pm}. \tag{32}$$

With $\alpha_L \equiv \alpha_{Ln} = \omega_{Ln}/v$, $k_0 \equiv k_{0n} = (K_c^2 - q^2)^{1/2}$, we find that

$$f_q^{\pm} = \frac{q^2}{(\alpha_L^2 - q^2)^2} \frac{1}{4} \ln \left[1 + \left(\frac{k_0}{q}\right)^2\right] \begin{cases} \cos^2(\alpha_L z_0/2), & m = \text{even} \\ \sin^2(\alpha_L z_0/2), & m = \text{odd}. \end{cases} \tag{33}$$

Bulk modes in different plates are completely decoupled. The summation over q extends to $m \leq N = [K_c z_0/\pi]$ ($k_0 \geq 0$), as explained in Sect. 2.

The interaction strength of bulk modes (32) increases with increasing film thickness z_0 or decreasing electron energy. In both cases, the interaction strength reaches the resonant points at $q = \alpha_L = \omega_{Ln}/v$, i. e. the resonance occurs when the electron velocity v is equal to the phase velocity ω_{Ln}/q of some bulk oscillation. This is in full agreement with the condition (18). The resonant points do not occur i) for very slow electron energies, such that $\omega_{Ln}/v > K_c$, because the electron velocity is less than a phase velocity of any bulk mode and ii) for very high electron energies, when $\omega_{Ln} z_0/\pi v < 1$, because the electron leaves the film too quickly, so the resonant effect could not occur.

In fact, A_B^n diverges at $q = \alpha_L$, as a consequence of our dispersionless bulk oscillational mode. As discussed in Sect. 2, this could be removed, which would yield the finite maxima at approximately the same positions ($q = \alpha_L$) in the EEL spectrum. However, such resonant effects, which explicitly show the discrete nature of bulk collective modes, have not been detected as yet in the EELS[20]. The reason might be that in transmission experiments, where the film thickness is well defined, (contrary to the electron penetration depth in the reflection case), neither the energy nor the film thickness are *continuously* changed in regions which are wide enough. One can easily find out that the resonance conditions

$$m = \frac{z_0 \omega_{Ln}}{\pi v} \approx 0.08 \frac{\omega_{Ln}(\text{eV})\, z_0(10^{-8}\,\text{cm})}{\sqrt{E_e(\text{eV})}} = 1,2,\ldots,N$$

are quite realistic. For instance, for an Al film 10^{-6} cm thick, we obtain resonances at $E_e \approx 15$ keV ($m = 1$), $E_e \approx 3.7$ keV ($m = 2$), $E_e \approx 1.6$ keV ($m = 3$), etc. The bulk plasmon dispersion and the relativistic correction to $v \sim \sqrt{E_e}$ can change these results only a little (the retardation effect does not affect the longitudinal frequency of bulk oscillations).

a) *The electron transmitted through a thin film*

For surface modes[7] in a thin film of thickness a, we find from (31) that

$$|\mathcal{J}_{\pm}(k)|^2 = 2\omega_P^2 \begin{cases} \operatorname{cth}(ka/2) \sin^2(\alpha_S^+ a/2) \\ \operatorname{th}(ka/2) \cos^2(\alpha_S^- a/2). \end{cases} \tag{34}$$

The contribution from bulk plasmons is given by (32, 33). Using the closure relation (7, I), one obtains

$$A_B^{(CR)} = A_0 \left\{ \ln \left[1 + \left(\frac{k_c}{a_L} \right)^2 \right] a - 2 \int_0^{k_c} \frac{\mathrm{d}k\, k^2}{(k^2 + a_L)^2} \sum_{s=\pm} |\mathcal{J}_s(k)|^2 \right\} \tag{35}$$

where

$$A_0 = \frac{e^2}{\hbar} \frac{1}{v^2} \frac{1}{2} \frac{\omega_P^2}{\omega_L}$$

and $|\mathcal{J}_s(k)|^2$ is given by (34) with $a_S^{\pm} \to a_L$.

As we have shown, the resonances at $q = a_L$ appear as a consequence of the discrete nature of the parameter q and are not obtained in the closure-relation approach. Here we shall briefly analyze the other discrepancies between our treatment and the closure-relation approach.

The qualitative difference appears between A_B and $A_B^{(CR)}$ for a very thin film ($a \sim K_c^{-1}$). In our model, bulk collective oscillations do not exist for $a < z' = \pi K_c^{-1} \approx 3\text{—}5 \times 10^{-8}$ cm. In the limit $a = z' + \eta$, $\eta \ll z'$, we find

$$A_B \approx A^0 \pi^2 \frac{\sin^2 (a_L z'/2)}{(a_L^2 z'^2 - \pi^2)^2} \eta' \sim \eta'.$$

At $a > z'$, only surface modes contribute. Their contribution vanishes ($A_S \sim a$) at $a \to 0$. When the closure relation is used, bulk collective oscillations appear in an arbitrarily thin film, as a consequence of $q_c \to \infty$ (one finds $A_B^{(CR)} \sim a^3$ at $a \to 0$).

In a very thick film ($a \gg K_c^{-1}$), we immediately find that $A_B^{(CR)} \sim a$. This is just the mean-free-path approximation, which should, obviously, hold when the contribution from surface excitations is negligible. To show that the same property ($A_B \sim a$) holds in our model, we assume $a \gg \omega_L/v$. According to (33), the main contribution to the spectrum arises from two terms for which

$$m_{\pm} = \frac{a}{\pi} \frac{\omega_L}{v} + \eta_{\pm}.$$

The factor $(a\omega_L/\pi v) \gg 1$ is generally between an even m_+ and an odd m_- number, so $|\eta_+| < 1$. Keeping only the leading terms in the sum (32), we find

$$A_B \approx \frac{1}{(2\pi)^2 \eta^2} A^0 a \ln \left(\frac{k_c v}{\omega_L} \right) \sim \frac{a}{\eta^2}$$

where $1/\eta^2 = \sin^2 (\omega_L a/2v)/\eta_-^2 + \cos^2 (\omega_L a/2v)/\eta_+^2$.

In the limit $a \to \infty$ (semiinfinite plate), the summation over m is replaced by the integration over q. This gives the bulk plasmon strength *per unit length* as follows:

$$A_B/l = A^0 \ln [1 + (k^0/a_L)^2] \tag{36}$$

where $l = \int_{-\infty}^{0} \mathrm{d}z$ and $k^0 = (k_c^2 - \alpha_L^2)^{1/2}$. The result obtained from the closure relation is

$$A_B/l = A^0 \ln [1 + (k_c/\alpha_L)^2]. \tag{37}$$

In the limit $k_c \to \infty$, both results coincide. However, for finite k_c, we find $\ln [1 + (k^0/\alpha_L)^2] = \ln (k_c/\alpha_L)^2$. This is in full agreement with the result of Chang and Langreth[16], who were the first to notice an inconsistency (k_c = finite, $q_c \to \infty$) in the closure-relation approach.

The surface term (31) remains finite ($|\mathcal{J}|^2 = \omega_P^2$), so that $A_S/l \to 0$ and the surface contribution can be neglected for a very thick plate.

Note that the results obtained for a thin film in the limit $a \to \infty$ are the same as those of a semiinfinite plate only if the plate is described by *two* degenerate surface modes, connected to both $z = 0$ and $z = -\infty$ surfaces. By describing the semiinfinite plate by only one surface mode, we would have implicity assumed that the electron could never pass through the $z = -\infty$ surface, and the strength of surface modes A_S would have been twice weaker.

Figure 6 shows the excitation probability of bulk and surface plasmons in the electron transmission through thin ($a = 25 \times 10^{-7}$ cm) Al and Mg films (Figs. 6a and 6b, respectively). The experimental curves[17] are given for an Al film 15×10^{-7} cm thick and for a Mg film 5×10^{-6} cm thick. Therefore, the ratio between the bulk and surface plasmon lines is roughly twice lower for Al (twice higher for Mg) than in Fig. 6. The second-order processes are much weaker than the first-order ones, since the electron energy is very high (E_e = 34 keV). Moreover, no second-order surface plasmon loss has been detected in the experiment.

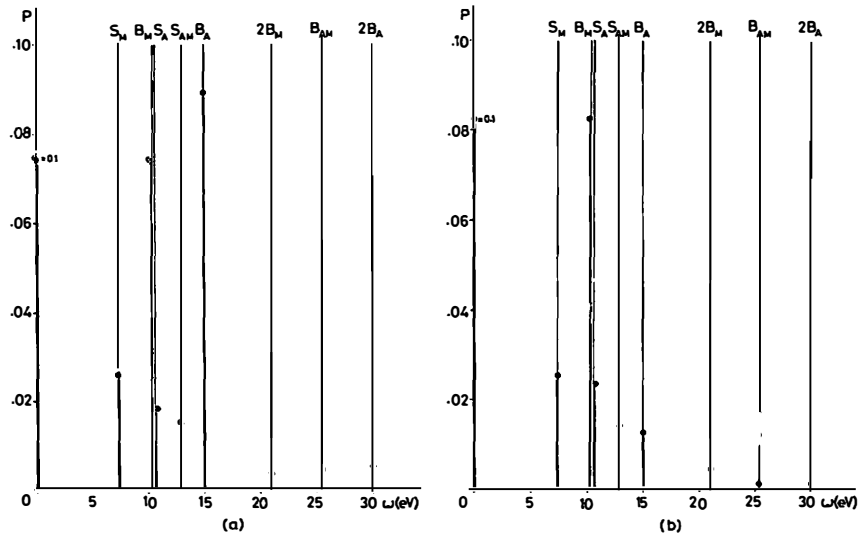

Fig. 6. Excitation probabilities of bulk (B) and surface (S) plasmons: the first- (B, S) and second-order ($2B$, $2S$, $B + S$) processes. We have chosen thin films: a) Al and b) Mg (ω_P = 10.5 eV, $K_c = 1.3 \times 10^8$ cm^{-1}).

b) *The electron transmitted through two thin films*

Full expressions for the interaction strengths of surface and bulk modes are given by Eqs. (29—31) and (32, 33), respectively. Contrary to surface modes, bulk modes are independent in each thin film, so the discussion of bulk modes in the preceding chapter was quite general.

In the limit of an infinitelly thick plate n, A_B^n diverges. The asymptotic behaviour of $\mathcal{J}_s(k)$ shows that A_S^s remains finite:

$$|\mathcal{J}_s(k \to \infty)|^2 \to \begin{cases} \omega_{P1}^2 & , \text{ if } (1+\varepsilon_1) \to 0 \\ \dfrac{4\omega_{P1}^2\,\omega_{P2}^2}{[\omega_{P1}^2(1+\varepsilon_1)^2 + \omega_{P2}^2(1+\varepsilon_2)^2]} & , \text{ if } (\varepsilon_1+\varepsilon_2) \to 0 \\ \omega_{P2}^2 & , \text{ if } (1+\varepsilon_2) \to 0. \end{cases}$$

It also shows that all surface modes connected with $z = a, 0, -b$ surfaces exhibit essentially the same coupling to the electron. This coupling is mainly independent of film thickness, except for very thin films.

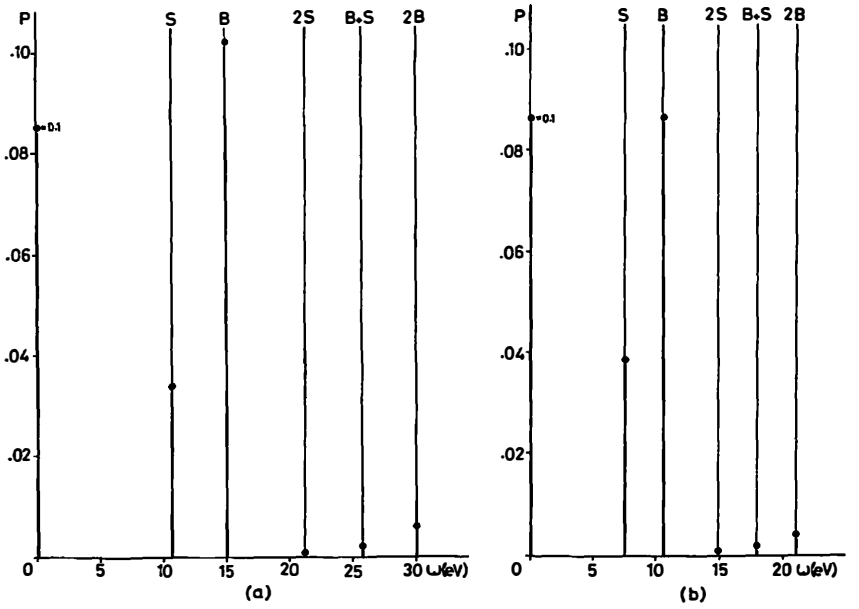

Fig. 7. Excitation probabilities of bulk (B) and surface (S) plasmons in an Al (A) + Mg (M) system. Here S_{AM} refers to the excitation of an Al-Mg interface plasmon, while B_{AM} denotes the excitation of bulk plasmons in both Al and Mg. We have chosen: a) $a = b = 25 \times 10^{-7}$ cm and b) a (Al) $= 5 \times 10^{7-}$ cm, b (Mg) $= 25 \times 10^{-7}$ cm, with $E_e = 34$ keV.

Figure 7 shows the EEL spectrum for electrons transmitted through thin Al + Mg sample. Comparison of Figs 6 and 7a shows that the first-order bulk losses in an Al + Mg system are a superposition of such losses in a thin Al and a thin Mg film. This is not true for surface losses, since the surface plasmon disper-

sion is drastically changed when Al and Mg films are put together. The new surface plasmon mode connected with the Al-Mg interface is detected. In the second-order bulk losses there is also a line describing the excitation of bulk plasmons in both Al and Mg films.

Figure 7b shows the Al-Mg system with an Al film five times thinner than in Fig. 7a. By comparing Figs. 7a and 7b, roughly the same reduction is obtained for the excitation probability of a bulk Al plasmon. All the results are in good agreement with experiment[17], with the following remarks: i) The asymptotic frequencies of surface Al and bulk Mg plasmons are very close, so these two lines are not separated in the experiment; ii) the assumed free Mg surface was put on a graphite substrate, which caused the lowering and shifting of the Mg surface plasmon line[17], due to the large imaginary part of the graphite dielectric constant.

Figure 8 shows the EEL spectrum ($E_e = 34$ keV) of a thin Al film covered on one surface ($z = -b$) with Al oxide. The figure shows only $P_1^S(\omega)$, since the oxidation does not affect the bulk plasmon line. With increasing Al_2O_3 thickness (b), the ω_- line is removed to lower frequencies. At $b \to \infty$, there are two well-separated spectral lines, the ω_+ line connected to the free Al surface ($\omega = \omega_P/\sqrt{2}$) and the ω_- line related to the Al-Al_2O_3 interface ($\omega = \omega_P/\sqrt{1+\varepsilon}$).

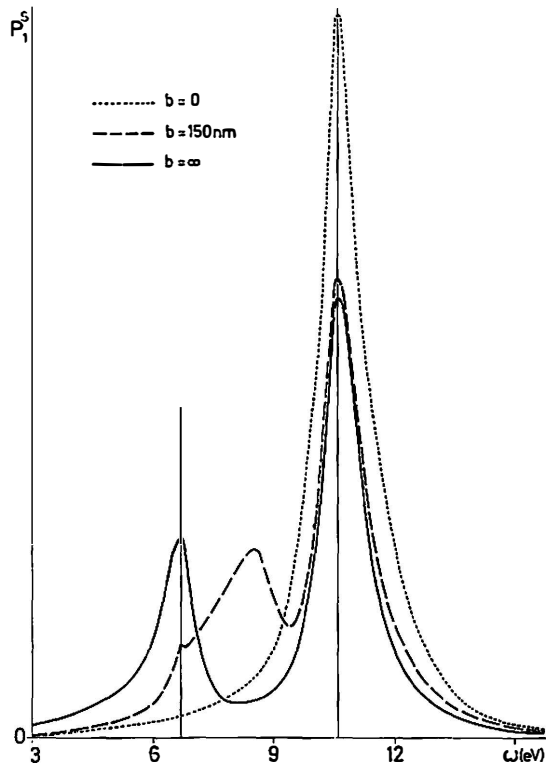

Fig. 8. The spectrum $P_1^S(\omega)$ of surface plasmon excitation $\omega_\pm(k)$ in a thin Al film ($a = 15 \times 10^{-7}$ cm), as a function of Al_2O_3 thickness b.

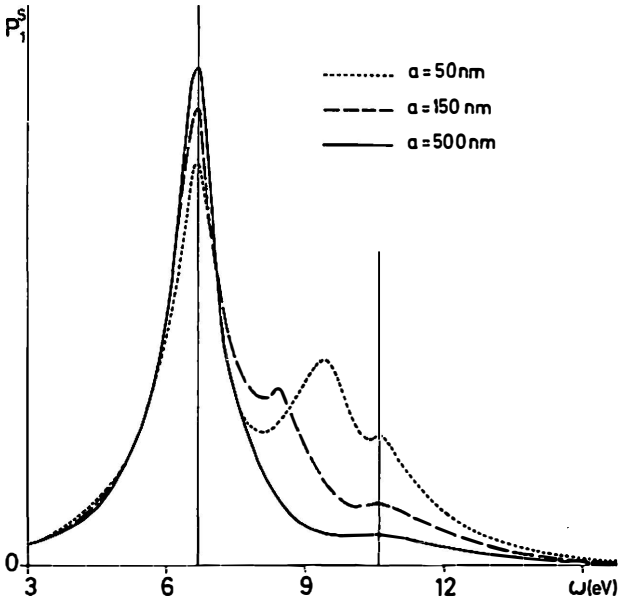

Fig. 9. The spectrum $F_1^S(\omega)$ of surface plasmon excitation $\omega_+(k)$ in a thin Al film ($b = 15 \times 10^{-7}$ cm) on an Al_2O_3 substrate ($z < -b$), as a function of Al_2O_3 film thickness a.

When the second Al surface is also oxidated, we obtain a system consisting of a thin Al_2O_3 film (a thick) adjacent to an Al film with an Al_2O_3 substrate. The only difference between this system and bilayer systems (I) is a change in boundary condition at $z = -b$, because there is an inert dielectric instead of a vacuum at $z < -b$. Therefore, only the dispersion curves $\omega_\pm(k)$ are changed[19]. The growth of Al_2O_3 at the $z = 0$ Al surface (Fig. 9) now removes the ω_+ mode to lower frequencies. At $a = 15 \times 10^{-8}$cm, we obtain a peak at $\hbar\omega_+ \approx 8.5$ eV, close to the experimental value $\hbar\omega \approx 8.9$ eV[19]. For thicker Al_2O_3 films ($a \approx 5 \times 10^{-7}$ cm), both modes $\omega_\pm$ contribute to the same line related to the Al-Al_2O_3 interface.

5. *Conclusions*

The general theory of collective oscillations in bilayer systems developed in I is applied in this paper to the EEL spectrum of electrons reflected from or transmitted through bilayer films. We show that a rather simple dielectric theory of collective oscillations (I), which could not give e. g. all details in the plasmon dispersion curve, is still quite satisfactory in describing some interesting experimental situations. This leads us to the following conclusions:

i) The trajectory approximation is valid when the energy of electrons is ten or more times higher than the energy of excited collective modes.

ii) The EELS of a bilayer system is described by the Poisson distribution if the system is not very thin and if the electron energy is not very high, i. e. the criteria are essentially the same as in a thin film[7].

iii) The finite bulk cutoff wave vector leads to some new interesting features of bulk collective oscillations. The closure-relation approach is not exact, and we obtain resonances in the EEL spectrum when the electron velocity is equal to the phase velocity of any excited bulk mode. Such resonances in the EELS would provide direct evidence for the discrete nature of bulk collective oscillations in a thin film, but they have not yet been verified experimentally.

iv) In electron reflection, we have found analytical expressions for the ratios of the dominant to interface mode interaction strengths. The probability of the electron-interface mode interaction decrease roughly exponentially with increassing thickness between the reflecting surface and the interface.

v) In electron transmission, the finite cutoff wave vector q_c plays an important role according to iii). In our model, bulk collective oscillations do not exist for films thinner than $\approx \pi q_c^{-1}$. Bulk collective oscillations in different films are independent of one another, and the probability of their excitations satisfies the Poisson distribution quite well.

References

1) R. H. Ritchie, Phys. Rev. **106** (1957) 874;

2) T. Fujiwara and K. Ohtaka, J. Phys. Soc. Japan **24** (1968) 1326;

3) E. A. Stern and R. Ferrel, Phys. Rev. **120** (1960) 130;

4) J. Heinrichs, Phys. Rev. **B5** (1972) 4792;

5) A. Otto, Z. Physik **185** (1956) 232;

6) S. Q. Wang and G. D. Mahan, Phys. Rev. **B6** (1972) 4517;

7) M. Šunjić and A. A. Lucas, Phys. Rev. **B3** (1971) 719;

8) E. Evans and D. L. Mills, Phys. Rev. **B5** (1972) 4126;

9) H. Ibach, J. Vac. Sci. & Technol. **9** (1971) 713;

10) H. Froitzheim, Topics in Current Physics **4** (1977) 205;

11) Z. Lenac and M. Šunjić, Fizika **13**(1981) 23;

12) C. J. Powell and J. B. Swann, Phys. Rev. **175** (1968) 972;

13) C. J. Powell and J. B. Swann, Phys. Rev. **118** (1960) 640;

14) R. L. Hengehold and F. L. Pedrotti, Phys. Rev. **B6** (1972) 2262;

15) L. J. Brillson, Phys. Rev. Lett. **38** (1977) 245;

16) J. J. Chang and D. C. Langreth, Phys. Rev. **B5** (1972) 3512;

17) C. Kunz, Z. Physik **196** (1966) 311;

18) H. Boersch, J. Geiger, A. Imbusch and N. Niedrig, Phys. Lett. **22** (1966) 146;

19) T. Kloos, Z. Physik **208** (1968) 77;

20) Notice that the optically detected size resonances in thin films (M. Anderegg, B. Feurbacher, and B. Fitton, Phys. Rev. Lett. **27** (1971) 1565) arise from the different physical mechanism, related to the intrinsic bulk plasmon dispersion.

POVRŠINSKI I VOLUMNI OPTIČKI FONONI I PLAZMONI U DVOSTRUKIM SLOJEVIMA. II. REFLEKSIJA I TRANSMISIJA ELEKTRONA

Z. LENAC i R. BRAKO

Institut »Ruđer Bošković«, Zagreb

i

M. ŠUNJIĆ

Prir.-mat. fakultet i Institut za fiziku Sveučilišta, Zagreb

UDK 538.975

Originalni znanstveni rad

U prethodnom članku razmatrali smo kolektivne titraje u dvostrukim slojevima. Sada želimo primijeniti dobivene rezultate na određivanje energetskih gubitaka elektrona pri refleksiji ili transmisiji na sistemu od dva različita sloja. Kod proučavanja refleksije elektrona analizirano je pobuđivanje površinskih titraja, a posebno utjecaj podloge na spektar energetskih gubitaka elektrona. Razmatrajući transmisiju elektrona, posebna pažnja je posvećena pobuđivanju volumnih titraja, kao i diskretnoj prirodi volumnih titraja u tankom sloju. Teorijski rezultati uspoređeni su s eksperimentima, i nađeno je dobro slaganje.